

GAUSSIAN IDEAL IMPULSIVE LOADING OF RIGID VISCOPLASTIC PLATES

Robert J. Hayduk
NASA Langley Research Center

ABSTRACT

The response of a thin, rigid viscoplastic plate subjected to a spatially axisymmetric Gaussian ideal impulse loading was studied analytically. The Gaussian ideal impulse distribution instantaneously imparts a Gaussian initial velocity distribution to the plate, except at the fixed boundary. The plate deforms with monotonically increasing deflections until the initial dynamic energy is completely dissipated in plastic work. The simply supported plate of uniform thickness obeys the von Mises yield criterion and a generalized constitutive equation for rigid, viscoplastic materials. For the small deflection bending response of the plate, neglecting the transverse shear stress in the yield condition and rotary inertia in the equations of dynamic equilibrium, the governing system of equations is essentially nonlinear. A proportional loading technique, known to give excellent approximations of the exact solution for the uniform load case, was used to linearize the problem and obtain analytical solutions in the form of eigenvalue expansions. The linearized governing equation required the knowledge of the collapse load of the corresponding static problem.

The effects of load concentration and an order of magnitude change in the viscosity of the plate material were examined while holding the total impulse constant. In general, as the load became more concentrated, the peak central velocity increased and the time for plate motion to cease increased. For the less viscous plate, these increases of velocity and time were more pronounced. The final plate profile became more conical as the load concentration increased, but did not approach the purely conical shape predicted for the point impulse by the rigid, perfectly plastic analysis with the Tresca yield criteria. Profiles of the less viscous plate were influenced more by the load concentration.

SYMBOLS

| | |
|----------------------------------------|----------------------------------------|
| A_n^I | series coefficient, equation (A6) |
| a | Gaussian distribution parameter |
| $B = \frac{\sqrt{3} \gamma}{2h}$ | plate geometry and material constant |
| \bar{C}_1, \bar{C}_2 | constants defined by equation (A5) |
| $F' = \frac{\sqrt{3} p'_0 R^2}{4 M_0}$ | nondimensional collapse load amplitude |

| | |
|-------------------------------------|---------------------------------------------------------------------------------|
| F | yield function |
| h | plate half-thickness |
| I | impulse per unit area amplitude at the plate center |
| $I' = \frac{IR^2}{M_0}$ | impulse parameter, sec |
| $J_p(x)$, $I_p(x)$ | Bessel function of the first kind of real and imaginary arguments, respectively |
| J'_2 | second invariant of the deviatoric stress tensor |
| \dot{k}_r , \dot{k}_ϕ | radial and circumferential curvature rates |
| \bar{k} | yield stress in simple shear |
| M_r , M_ϕ | radial and circumferential bending-moment resultants |
| \bar{M}_r , \bar{M}_ϕ | radial and circumferential bending-moment resultants at initial yield |
| $M_o = \sigma_o h^2$ | yield moment of the plate |
| $m = \frac{M_r}{M_o}$ | nondimensional radial bending-moment resultant |
| $n = \frac{M_\phi}{M_o}$ | nondimensional circumferential bending-moment resultant |
| p'_o | pressure amplitude at the plate center at collapse |
| $\bar{p}'_o = \frac{p'_o R^2}{M_o}$ | nondimensional pressure amplitude at the plate center at collapse |
| Q | shear stress resultant |
| $q = \frac{RQ}{M_o}$ | nondimensional shear stress resultant |
| R | plate radius |
| r | radial coordinate |
| s_{ij} | deviator stress tensor |

| | |
|---------------------------------|--------------------------------------------------------------|
| \bar{s}_{ij} | deviator stress tensor at initial yield |
| t | time |
| t_f | time for motion to cease |
| $u(\rho, t)$ | dynamic component of velocity |
| $U(\rho)$ | steady component of velocity |
| v | initial velocity |
| v | nondimensional plate velocity |
| w | transverse deflection of the plate |
| z | transverse coordinate |
| $\alpha = \frac{\mu BR^4}{M_0}$ | plate geometry and material constant, sec |
| $\beta = a^2 R^2$ | nondimensional Gaussian shape parameter |
| γ, γ^0 | material constants |
| ∇^2, ∇^4 | harmonic and biharmonic operators in cylindrical coordinates |
| δ | final center deflection |
| \dot{e}_{ij} | strain rate tensor |
| λ_n | eigenvalues determined from equation (A7) |
| ρ | mass density per unit area of the plate |
| r | nondimensional radial coordinate |
| σ_{ij} | stress tensor |
| σ_0 | yield stress in simple tension |
| (F) | function defined by equation (3) |
| θ | circumferential coordinate |
| (λ_n, β) | function defined by equation (A13) |
| (λ_n, ρ, β) | function defined by equation (A12) |

INTRODUCTION

This paper presents the results of an analysis of the small-deflection bending response of a simply supported circular plate of rigid, viscoplastic material subjected to a spatially axisymmetric Gaussian ideal impulse. The effects of load concentration and an order of magnitude change in the viscosity of the plate material are examined while holding the total impulse constant. Approximate expressions are developed for the time at which plate motion ceases, the final shape of the plate, and the final central displacement.

Although there have been a number of papers (refs. 1, 2, 3) which permit a time variation of the load, there have been few papers which consider a radial variation other than linear (refs. 3, 4). The only general spatial distribution of load which has received significant analytical attention is the Gaussian distribution. By varying a single parameter, this general distribution can span the extremes from the point load to the uniformly distributed load. This versatility was recognized by Sneddon (ref. 5) who approximated the dynamic loading of a projectile on a thin, infinite elastic plate by a Gaussian distribution of pressure. Madden (ref. 6), in his study of shielding of space vehicle structures against meteoroid penetration, related the meteoroid-shield debris loading of the main vehicle wall to a Gaussian initial velocity distribution. The first study of this loading on a plastic plate was by Thomson (ref. 7). He obtained the solution of a rigid, perfectly plastic plate of material obeying the Tresca yield condition subjected to an initial impulse of Gaussian distribution. Weidman (ref. 2), in considering the response of simply supported circular plastic plates to distributed time-varying loadings, presented an example case of a radial Gaussian distribution of pressure with an exponential decay. The plate material was also rigid, perfectly plastic obeying the Tresca yield conditions.

A generalized constitutive equation for rigid, viscoplastic materials is presented in the next section. Material elasticity is neglected in order to simplify the analysis, as is frequently done in theoretical investigations of dynamic plastic response of structures. Rigid-plastic analyses are generally believed to be valid when the dynamic energy is considerably larger than the maximum energy which could be absorbed in a wholly elastic manner and the duration of loading is short compared with the fundamental period of vibration.

LINEARIZATION OF THE GENERALIZED CONSTITUTIVE EQUATIONS

FOR RIGID, VISCOPLASTIC MATERIALS

Perzyna (ref. 8) developed a generalized constitutive equation for rate sensitive plastic materials by incorporating a general function in the relationship to take the place of the yield function as used by previous researchers (Hohenemser and Prager, ref. 9; and Prager, ref. 10). Utilizing the definition of the second invariant of the stress deviator, $J_2' = \frac{1}{2} S_{ij} S_{ij}$, the yield function is expressed as

$$F = \frac{J_2^{1/2}}{k} - 1 \quad (1)$$

where S_{ij} is the stress deviator tensor and k is the yield stress. The generalized constitutive equation proposed by Perzyna is

$$\dot{\varepsilon}_{ij} = \gamma^0 \Phi(F) \frac{\partial F}{\partial \sigma_{ij}} \quad (2)$$

where $\dot{\varepsilon}_{ij}$ is the strain rate tensor,

$$\begin{aligned} \Phi(F) &= 0 \quad \text{if } F \leq 0 \\ \Phi(F) &\neq 0 \quad \text{if } F > 0 \end{aligned} \quad (3)$$

and γ^0 denotes a physical constant of the material.

Perzyna (ref. 11) has shown that the generalized constitutive equation for viscoplastic materials reduces to the constitutive equations of an incompressible, perfectly plastic material first considered by von Mises and to the flow law of perfect plasticity theory. As in the theory of perfectly plastic solids, convexity of the subsequent dynamic loading surfaces and orthogonality of the inelastic strain-rate vector to the yield surface follow from Drucker's postulates defining a stable, inelastic material with inclusion of time-dependent terms (Perzyna, ref. 8).

A method of linearizing boundary-value problems in the theory of viscoplastic solids is described by Wierzbicki in reference 12. In this method, as shown graphically in figure 1, the concept of proportional loading is used to relate the state of stress \bar{S}_{ij} on the initial yield surface $F = 0$ to subsequent states of stress, namely, proportional loading requires the direction cosine tensor of the state of stress in deviatoric space to be independent of time:

$$\frac{S_{ij}}{J_2^{1/2}} = \frac{\bar{S}_{ij}}{k} \quad (4)$$

This is a reasonable approximation for axisymmetrically loaded simply supported circular plates because the plate center and boundary are automatically proportionally loaded, that is, the bending moments must always be equal at the plate center and the circumferential bending moment must always be zero at the plate boundary.

Utilizing equation (4), the generalized constitutive equation (2) becomes

$$\dot{\varepsilon}_{ij} = \frac{\gamma}{k} \Phi \left(\frac{S_{ij}}{\bar{S}_{ij}} - 1 \right) \bar{S}_{ij} \quad (5)$$

where the viscosity constant $\gamma = \gamma^0/2k$. For this analysis, the linear form

$$\Phi(F) = F \quad (6)$$

is chosen. This simplified constitutive equation still is nonlinear in stress. However, in the solution of dynamical plate and rotationally symmetric shell problems, the constitutive equation (5) with the linear function $\Phi(F) = F$ produces full linearization of the governing equations.

For the problem of a uniformly loaded, simply supported circular plate with $\Phi(F) = F$, Wierzbicki (ref. 12) has shown that the approximate solution obtained using the proportional loading hypothesis agrees very well with a numerical finite-difference solution of the exact equations. The solution of the linearized problem also agrees well with experimental data on impulsively loaded plates by Florence (ref. 13).

For the linear function equation (5) becomes

$$\dot{\varepsilon}_{ij} = \frac{\gamma}{k} (S_{ij} - \bar{S}_{ij}) \quad (7)$$

where equation (7) is really a flow relation for a given structure rather than a constitutive equation describing a given material (ref. 14).

GOVERNING EQUATIONS, BOUNDARY AND INITIAL CONDITIONS

A Gaussian ideal impulse is suddenly applied to the entire surface of a rigid, viscoplastic plate of radius R and thickness $2h$ resulting in an initial velocity distribution described by

$$V(r, 0) = \frac{I}{\mu} e^{-a^2 r^2} \quad (8)$$

where I is the impulse per unit area at the center of the plate and μ is the mass density per unit area of the plate middle surface. The boundary of the plate at $r = R$ is simply supported. The geometry of the plate and initial velocity are shown in figure 2.

The parameter a in the distribution function is a shape parameter which controls the distribution of the impulse. For $a = 0$ equation (8) describes a uniform impulse; and as $a \rightarrow \infty$, $I \rightarrow \infty$ equation (8) describes a point impulse at the plate center.

The internal forces and moments acting on a typical plate element are shown in figure 3. If rotary inertia is neglected, but transverse inertia taken into account, the equations of motion are

$$\frac{\partial}{\partial r} (rQ) = \mu r \frac{\partial^2 w}{\partial t^2}$$

$$\frac{\partial}{\partial r} (rM_r) - M_\phi = rQ$$
(9)

Utilizing the Love-Kirchoff hypotheses, the curvature-rate-moment relations, derived from the linearized constitutive equation, equation (7), are

$$\dot{K}_r = \frac{B}{M_o} [(2M_r - M_\phi) - (2\bar{M}_r - \bar{M}_\phi)]$$
(10)

$$\dot{K}_\phi = \frac{B}{M_o} [(2M_\phi - M_r) - (2\bar{M}_\phi - \bar{M}_r)]$$

where $B = \sqrt{3} \gamma / 2h$. \bar{M}_r and \bar{M}_ϕ are moments satisfying for any r the equation of the initial yield surface

$$M_r^2 - M_r M_\phi + M_\phi^2 = M_o^2$$
(11)

$M_o = \sigma_o h^2$ is the yield moment of the plate material and σ_o is the yield stress in simple tension.

For small deflections of the plate the curvature rates \dot{K}_r and \dot{K}_ϕ are related to the deflection rate \dot{w} by

$$\dot{K}_r = - \frac{\partial^2 \dot{w}}{\partial r^2}; \quad \dot{K}_\phi = - \frac{1}{r} \frac{\partial \dot{w}}{\partial r}$$
(12)

Equations (9), (10), and (12) form a linear parabolic system of partial differential equations with six unknown functions — M_r , M_ϕ , Q , w , K_r , and K_ϕ — plus the unknown static moment distribution \bar{M}_r and \bar{M}_ϕ .

By eliminating all unknowns except \dot{w} , the system of governing equations can be reduced to the single, fourth-order equation

$$\frac{2M_o}{3B} \nabla^4 \dot{w} + \mu \frac{\partial \dot{w}}{\partial t} = \frac{1}{r} \frac{\partial}{\partial r} [\frac{\partial}{\partial r} (r\bar{M}_r) - \bar{M}_\phi]$$
(13)

where

$$\nabla^4 = \left[\frac{\partial^2}{\partial r^2} + \frac{1}{r} \frac{\partial}{\partial r} \right] \left[\frac{\partial^2}{\partial r^2} + \frac{1}{r} \frac{\partial}{\partial r} \right]$$

The right-hand side of equation (13) represents the internal force distribution at the initiation of collapse in the static case.

Let p'_o denote the static load-carrying capacity of the plate, then the right-hand side of equation (13) can be replaced by $-p'_o e^{-a^2 r^2}$ and the governing equation becomes

$$\frac{2M_o}{3B} \nabla^4 w + \mu \frac{\partial \dot{w}}{\partial t} = - p'_o e^{-a^2 r^2} \quad (14)$$

This method of solution, proposed by Wierzbicki (ref. 12), has the important property of replacing the unknown static moment distribution \bar{M}_r and \bar{M}_ϕ , whose explicit formulas are not known for the von Mises yield condition, by the static load-carrying capacity p'_o . Thus, the need for explicit formulas has been reduced to finding the value of a constant, p'_o , corresponding to a particular value of the shape parameter, a . The determination of the load-carrying capacity, p'_o , of a circular plate under a Gaussian distribution of pressure is presented in reference 15.

Define the dimensionless quantities

$$m = \frac{M_r}{M_o}, \quad n = \frac{M_\phi}{M_o}, \quad q = \frac{RQ}{M_o}$$

$$\rho = \frac{r}{R}, \quad \beta = a^2 R^2 \quad (15)$$

$$v = \frac{1}{BR^2} \frac{\partial w}{\partial t}, \quad F' = \frac{\sqrt{3} p'_o R^2}{4 M_o}$$

and let $\nabla^2 = \frac{\partial^2}{\partial \rho^2} + \frac{1}{\rho} \frac{\partial}{\partial \rho}$. Then the final form of the governing equation, equation (14), is

$$\nabla^4 v + \frac{3}{2} \alpha \frac{\partial v}{\partial t} = - 2 \sqrt{3} F' e^{-\beta \rho^2} \quad (16)$$

where $\alpha = \mu BR^4 / M_o$.

The boundary conditions of the simply supported plate are

$$m = n, \quad q = 0 \quad \text{at} \quad \rho = 0$$

(17)

$$v = m = 0 \quad \text{at} \quad \rho = 1$$

Using equations (10), (12), and (9), equations (17), in terms of rate of deflection become

$$\begin{aligned} \lim_{\rho \rightarrow 0} \left(\frac{\partial^2 v}{\partial \rho^2} - \frac{1}{\rho} \frac{\partial v}{\partial \rho} \right) &= 0; \quad \lim_{\rho \rightarrow 0} \left(\frac{\partial^3 v}{\partial \rho^3} + \frac{1}{\rho} \frac{\partial^2 v}{\partial \rho^2} - \frac{1}{\rho^2} \frac{\partial v}{\partial \rho} \right) = 0; \\ 2 \frac{\partial^2 v}{\partial \rho^2} + \frac{\partial v}{\partial \rho} \Big|_{\rho=1} &= 0; \quad v(1, t) = 0 \end{aligned} \quad (18)$$

For the Gaussian ideal impulsive loading the plate is initially flat and the initial velocity has a Gaussian distribution

$$w(\rho, 0) = 0; \quad v(\rho, 0) = \frac{I'}{\alpha} e^{-\beta\rho^2} \quad (19)$$

$$\text{where } I' = \frac{IR^2}{M_0}.$$

RESULTS AND DISCUSSION

The solution to the governing equation, equation (16), with associated boundary and initial conditions, equations (18) and (19) are presented in the Appendix. The effects of load distribution and plate viscosity on plate response are examined in this section while holding the total impulse constant.

The impulse amplitude, $I' = IR^2/M_0$, sec, at the plate center is related to the total impulse, I^T , and distribution parameter, β , by the relation

$$I' = \frac{I^T}{\pi M_0} \left(\frac{\beta}{1 - e^{-\beta}} \right) \quad (20)$$

For comparison purposes the total impulse is held constant at $\frac{I^T}{\pi M_0} = 1 \times 10^{-3}$ sec. The impulse becomes more concentrated at the center of the plate as β is increased and the amplitude grows almost linearly as β becomes large. For $\beta = 0$, the impulse has a uniform distribution.

The graphical results were obtained by programming the solution (equations (A14) and (A15)) and summing the series term-by-term. The rapidly convergent series with $1/\lambda_n^5$ and $1/\lambda_n^9$ factors did not present any computational difficulties; however, the last series in the velocity expression equation (A14)

has a $1/\lambda_n$ factor and prohibited the calculation of velocity-time histories for small β and t . For $t = 0$ the series is slowly convergent.

A representative plot of the plate central velocity is shown in figure 4 for $\beta = 10$ and viscosity parameter $\alpha = 1 \times 10^{-2}$ sec. The initial central velocity is seen to rapidly decline during the first 0.025 msec after which the velocity more slowly tends to zero.

The plate is seen to deform monotonically with increasing deflection until the initial dynamic energy is completely dissipated in plastic work and the plate comes to rest. The deformed profiles of the plate at rest are shown in figure 5 for two values of α (1×10^{-2} , 1×10^{-3}) and various values of β . The profile becomes more conical as the impulse becomes more concentrated and the profiles of the less viscous plate ($\alpha = 1 \times 10^{-2}$ sec) exhibit a wider variation, thus are influenced more by the shape parameter β than are those for the $\alpha = 1 \times 10^{-3}$ sec case.

Approximations

An approximation to the deflection of the plate is obtained from equation (A15) by retaining only the first terms of series and using the approximation

$$\begin{aligned} \bar{C}_1 + \bar{C}_2 \rho^2 + \frac{1}{2\beta} e^{-\beta\rho^2} + \left(\frac{1}{\beta} + \rho^2\right) \sum_{n=1}^{\infty} \frac{(-1)^n (\beta\rho^2)^n}{(2n) n!} \\ \approx -\frac{16\beta}{3} \frac{1}{\lambda_1^5} \psi(\lambda_1, \rho, \beta) \end{aligned}$$

The result is

$$\begin{aligned} \frac{1}{BR^2} w(\rho, t) = -\frac{\sqrt{3} F'}{4\beta} \left[\bar{C}_1 + \bar{C}_2 \rho^2 + \frac{1}{2\beta} e^{-\beta\rho^2} + \left(\frac{1}{\beta} + \rho^2\right) \sum_{n=1}^{\infty} \frac{(-1)^n (\beta\rho^2)^n}{(2n) n!} \right] \\ \left\{ \left(1 - e^{-\frac{2\lambda_1^4}{3\alpha} t} \right) \left(\frac{3\alpha}{2\lambda_1^4} + \frac{\sqrt{3} I'}{4F'} \right) - t \right\} \quad (21) \end{aligned}$$

An approximate expression for the time for motion to cease can be obtained by setting the derivative of the approximate displacement expression to zero,

that is, $\frac{\partial w}{\partial t} \Big|_{t_f} = 0$, is

$$t_f = \frac{3\alpha}{2\lambda_1^4} \ln \left(1 + \frac{\lambda_1^4 I'}{2\sqrt{3} F' \alpha} \right) \quad (22)$$

Equation (22) is plotted in figure 6 for $0 \leq \beta \leq 100$ and several values of α . Equation (22) is an implicit function of β since I' and F' vary with β . The effect of β diminishes after an initial rapid rise of t_f with increasing β . The symbolized points represent computed times using the complete equation for the velocity, equation (A14). Equation (22) is a very good approximation for the case $\alpha = 1 \times 10^{-3}$ sec. However, except for small values of β , the approximation is poor for the $\alpha = 1 \times 10^{-2}$ sec case.

For $\alpha \rightarrow \infty$ equation (22) limits to

$$t_f = \frac{\sqrt{3} I'}{4F'} \quad (23)$$

$$= \frac{I}{\bar{p}_o'}$$

and represents the rigid, perfectly plastic case ($\gamma \rightarrow \infty$) with the von Mises yield condition. Equation (23) has the same form as Wang's (ref. 16) result for the uniform ideal impulse problem using the Tresca yield condition for a rigid perfectly plastic material. However, equation (23) gives slightly smaller values of t_f since $\bar{p}_o' = 6.51$ for the von Mises yield condition rather than 6 in the case of the Tresca yield condition.

The curve labeled Tresca, r.p.p. was obtained from the results of reference 7 where a simply supported circular plate of rigid, perfectly plastic material obeying the Tresca yield condition and associated flow rule was analyzed for a general Gaussian ideal impulse loading. For small β the two curves differ only slightly, but as β grows larger and the impulse becomes more concentrated, the two analyses predict drastically different times for the plate motion to cease. The Tresca yield condition predicts very large times for plate motion to cease, whereas the von Mises yield condition predicts more realistic times for concentrated loads.

The substitution of equation (22) for t_f into equation (21) provides an approximate expression for the final plate displacements:

$$\frac{1}{BR^2} w(\rho, t) = -\frac{\sqrt{3} F'}{4\beta} \left[\bar{C}_1 + \bar{C}_2 \rho^2 + \frac{1}{2\beta} e^{-\beta\rho^2} + \left(\frac{1}{\beta} + \rho^2 \right) \sum_{n=1}^{\infty} \frac{(-1)^n (\beta\rho^2)^n}{(2n) n!} \right]$$

$$\left\{ \frac{\sqrt{3} I'}{4F'} - \frac{3\alpha}{2\lambda_1^4} \ln \left(1 + \frac{\lambda_1^4 I'}{2\sqrt{3} F' \alpha} \right) \right\} \quad (24)$$

and for the final center displacement $\delta(0, t_f) = w(0, t_f)$:

$$\frac{\mu R^2}{\alpha M_0} \delta(0, t_f) = -\frac{\sqrt{3} F'}{4\beta} \left(\bar{C}_1 + \frac{1}{2\beta} \right) \left\{ \frac{\sqrt{3} I'}{4F'} - \frac{3\alpha}{2\lambda_1^4} \ln \left(1 + \frac{\lambda_1^4 I'}{2\sqrt{3} F' \alpha} \right) \right\} \quad (25)$$

Equation (25) is plotted as a function of β for the two values of α in figure 7. The approximations are in excellent agreement with the points computed from the exact equations for both $\alpha = 1 \times 10^{-3}$ sec and 1×10^{-2} sec, even though the t_f -approximations for the larger α were poor for large β as shown in figure 6. The nondimensional central displacements are shown smaller for the $\alpha = 1 \times 10^{-2}$ sec case when, in reality the real displacements are larger than for the $\alpha = 1 \times 10^{-3}$ sec case. This is caused by α being in the denominator of the expression for the nondimensional central displacement.

Profiles obtained from the approximation, equation (24), were compared with profiles obtained from the exact equation. For $\alpha = 1 \times 10^{-3}$ sec, the differences between the approximate and exact profiles were negligibly small for the entire range of β considered, 10^{-3} to 10,000. However, for the less viscous plates, $\alpha = 1 \times 10^{-2}$ sec, the differences were not negligible and the approximation, equation (23), should therefore be restricted accordingly.

CONCLUDING REMARKS

A thin, simply supported rigid, viscoplastic plate subjected to a Gaussian ideal impulse has been analyzed within the realm of small deflection bending theory. The plate material obeys the von Mises yield criteria and constitutive equations due to Perzyna (ref. 11). These considerations lead, essentially, to nonlinear equations governing the dynamic response of the thin plate. A proportional loading hypothesis, proposed by Wierzbicki (ref. 12) and shown to be an excellent approximation of the exact solution for the uniform load case, was used to linearize the problem and obtain analytical solutions in the form of eigenvalue expansions. The linearized governing equation on the velocity of the plate required the knowledge of the collapse load of the corresponding static problem, that is, the collapse load for the specific load distribution parameter, β .

The effects of impulse concentration and an order of magnitude change in the viscosity of the plate material were examined while holding the total impulse constant. In general, as the impulse became more concentrated, the peak central velocity increased and the time for plate motion to cease increased. For the less viscous plate material, these increases of velocity and time, t_f , for plate motion to cease are more pronounced. The final plate profile became more conical as the load concentration increased, but did not approach the purely conical shape predicted by the rigid, perfectly plastic analysis with the Tresca yield condition for a point impulse. As the viscosity of the plate decreases, the shape parameter has more effect on the final deformed plate profiles.

Approximate expressions were developed for the time at which plate motion ceases, t_f , the final shape of the plate, and the final central displacement. Comparisons with the series solution indicated that the approximations were excellent for the $\alpha = 1 \times 10^{-3}$ sec case. The approximation for the final central deflection was good for the entire range of shape parameter β , the other approximations were limited in usefulness.

APPENDIX

SOLUTION OF EQUATION (16) BY EIGENVALUE EXPANSION*

Since the right-hand side of equation (16) is not a function of time, it can be solved by means of an eigenvalue expansion method. Substitution of

$$v(\rho, t) = u(\rho, t) + U(\rho) \quad (A1)$$

into equation (16) results in

$$\nabla^4 u(\rho, t) + \frac{3}{2} \alpha \frac{\partial u(\rho, t)}{\partial t} + \nabla^4 U(\rho) = -2\sqrt{3} F' e^{-\beta\rho^2}$$

which separates into

$$\nabla^4 u + \frac{3}{2} \alpha \frac{\partial u}{\partial t} = 0 \quad (A2)$$

and

$$\nabla^4 U = -2\sqrt{3} F' e^{-\beta\rho^2} \quad (A3)$$

Equation (A3) is the same as equation (16) except for the absence of the inertia term. Thus, $U(\rho)$ is an equilibrium solution of equation (16) with the same boundary conditions, equations (17).

The solution to equation (A3) satisfying the boundary conditions, equations (18), is

$$U(\rho) = \frac{\sqrt{3}}{4\beta} F' \left\{ \bar{C}_1 + \bar{C}_2 \rho^2 + \frac{1}{2\beta} e^{-\beta\rho^2} + \left(\frac{1}{\beta} + \rho^2 \right) \sum_{m=1}^{\infty} \frac{(-1)^m (\beta\rho^2)^m}{(2m) m!} \right\} \quad (A4)$$

where

$$\bar{C}_1 = \frac{1}{6\beta} - \frac{7}{6} - \frac{2}{3\beta} e^{-\beta} - \frac{1}{\beta} \sum_{m=1}^{\infty} \frac{(-1)^m \beta^m}{(2m) m!} \quad (A5)$$

* For more details, the reader can consult "Gaussian Impulsive Loading of Rigid Viscoplastic Plates," by R. J. Hayduk, Ph. D. Thesis, Virginia Polytechnic Institute and State University, Blacksburg, Virginia, 1972.

and

$$\bar{c}_2 = -\frac{1}{6\beta} + \frac{7}{6} - \frac{1}{6\beta} e^{-\beta} - \sum_{m=1}^{\infty} \frac{(-1)^m \beta^m}{(2m) m!}$$

A general solution due to Wierzbicki (ref. 12) satisfying equation (A2) and all prescribed boundary conditions can be written in the form

$$u(\rho, t) = \sum_{n=1}^{\infty} A_n^I [I_0(\lambda_n) J_0(\lambda_n \rho) - J_0(\lambda_n) I_0(\lambda_n \rho)] e^{-(2\lambda_n^4/3\alpha)t} \quad (A6)$$

where $J_0(x)$ and $I_0(x)$ denote the Bessel functions of the first kind of real and imaginary arguments. The solution (A6) identically satisfies boundary conditions (18 a, b, and d). The eigenvalues, λ_n , are roots of the following transcendental equation stemming from the boundary condition (18c) of zero bending moment at the plate edge

$$I_0(\lambda_n) J_1(\lambda_n) + I_1(\lambda_n) J_0(\lambda_n) - 4\lambda_n I_0(\lambda_n) J_0(\lambda_n) = 0 \quad (A7)$$

The only remaining unknowns in the solution are the series coefficients A_n^I . These coefficients are evaluated from the initial condition (19), that is,

$$v(\rho, 0) = u(\rho, 0) + U(\rho) = \frac{I'}{\alpha} e^{-\beta\rho^2}$$

Thus,

$$u(\rho, 0) = -U(\rho) + \frac{I'}{\alpha} e^{-\beta\rho^2} \quad (A8)$$

and after substituting equation (A6) for $u(\rho, 0)$ there results

$$\sum_{n=1}^{\infty} A_n^I [I_0(\lambda_n) J_0(\lambda_n \rho) - J_0(\lambda_n) I_0(\lambda_n \rho)] = -U(\rho) + \frac{I'}{\alpha} e^{-\beta\rho^2} \quad (A9)$$

The coefficients A_n^I can be determined from (A9) by virtue of the orthogonality of the system $[I_0(\lambda_n) J_0(\lambda_n \rho) - J_0(\lambda_n) I_0(\lambda_n \rho)]$ on the interval $[0, 1]$ where ρ is used as a weighting function. Therefore, coefficients A_n^I can be determined as

$$A_n^I = -\frac{\int_0^1 (\rho U(\rho) - \rho \frac{I'}{\alpha} e^{-\beta\rho^2}) [I_0(\lambda_n) J_0(\lambda_n \rho) - J_0(\lambda_n) I_0(\lambda_n \rho)] d\rho}{\int_0^1 \rho [I_0(\lambda_n) J_0(\lambda_n \rho) - J_0(\lambda_n) I_0(\lambda_n \rho)]^2 d\rho} \quad (A10)$$

where $U(\rho)$ is defined by equation (A4). The resulting coefficients are

$$A_n^I [I_o(\lambda_n)J_o(\lambda_n\rho) - J_o(\lambda_n)I_o(\lambda_n\rho)] = [\frac{4}{\sqrt{3}} F' \frac{1}{\lambda_n^5} + \frac{2}{3} \frac{I'}{\alpha} \frac{1}{\lambda_n}] \psi(\lambda_n, \rho, \beta) \quad (A11)$$

where the functions $\psi(\lambda_n, \rho, \beta)$ are defined by the relation

$$\frac{16\beta}{3\lambda_n^5} \psi(\lambda_n, \rho, \beta) = \phi(\lambda_n, \beta) [I_o(\lambda_n)J_o(\lambda_n\rho) - J_o(\lambda_n)I_o(\lambda_n\rho)] \quad (A12)$$

with

$$\begin{aligned} & \frac{1}{\lambda_n} \bar{C}_1 I_o(\lambda_n) J_1(\lambda_n) - \frac{1}{\lambda_n} \bar{C}_1 J_o(\lambda_n) I_1(\lambda_n) + \bar{C}_2 I_o(\lambda_n) \left[\frac{1}{\lambda_n} J_1(\lambda_n) - \frac{4}{\lambda_n^3} J_1(\lambda_n) + \frac{2}{\lambda_n^2} J_o(\lambda_n) \right] \\ & - \bar{C}_2 J_o(\lambda_n) \left[\frac{1}{\lambda_n} I_1(\lambda_n) - \frac{2}{\lambda_n^2} I_o(\lambda_n) + \frac{4}{\lambda_n^3} I_1(\lambda_n) \right] + \frac{1}{2\beta} I_o(\lambda_n) \int_0^1 x e^{-\beta x^2} J_o(\lambda_n x) dx \\ & - \frac{1}{2\beta} J_o(\lambda_n) \int_0^1 x e^{-\beta x^2} I_o(\lambda_n x) dx + I_o(\lambda_n) \int_0^1 x (\frac{1}{\beta} + x^2) \sum_{m=1}^{\infty} \left[\frac{(-1)^m (\beta x^2)^m}{(2m)m!} \right] J_o(\lambda_n x) dx \\ & - J_o(\lambda_n) \int_0^1 x (\frac{1}{\beta} + x^2) \sum_{m=1}^{\infty} \left[\frac{(-1)^m (\beta x^2)^m}{(2m)m!} \right] I_o(\lambda_n x) dx \\ \phi(\lambda_n, \beta) = & \frac{-}{I_o(\lambda_n) J_o(\lambda_n) \{2\lambda_n [I_o(\lambda_n) J_1(\lambda_n) - I_1(\lambda_n) J_o(\lambda_n)] - 3I_o(\lambda_n) J_o(\lambda_n)\}} \quad (A13) \end{aligned}$$

When equations (A4) and (A6) are summed and equation (A11) is used, the complete solution becomes

$$\begin{aligned} v(\rho, t) = & \frac{\sqrt{3}}{4\beta} F' \left\{ \bar{C}_1 + \bar{C}_2 \rho^2 + \frac{1}{2\beta} e^{-\beta \rho^2} + (\frac{1}{\beta} + \rho^2) \sum_{n=1}^{\infty} \frac{(-1)^n (\beta \rho^2)^n}{(2n)n!} \right\} \\ & + \frac{4}{\sqrt{3}} F' \sum_{n=1}^{\infty} \frac{1}{\lambda_n^5} \psi(\lambda_n, \rho, \beta) e^{-(2\lambda_n^4/3\alpha)t} + \frac{2}{3} \frac{I'}{\alpha} \sum_{n=1}^{\infty} \frac{1}{\lambda_n} \psi(\lambda_n, \rho, \beta) e^{-(2\lambda_n^4/3\alpha)t} \quad (A14) \end{aligned}$$

The displacement of the plate is determined by integrating (A14) with respect to time. Taking the initial condition of zero displacement into account, the displacement becomes

$$\begin{aligned}
 \frac{1}{BR^2} w(\rho, t) = & \frac{\sqrt{3}}{4\beta} F't \left[\bar{c}_1 + \bar{c}_2 \rho^2 + \frac{1}{2\beta} e^{-\beta\rho^2} + \left(\frac{1}{\beta} + \rho^2 \right) \sum_{n=1}^{\infty} \frac{(-1)^n (\beta\rho^2)^n}{(2n) n!} \right] \\
 & + \frac{4}{\sqrt{3}} F' \frac{3\alpha}{2} \sum_{n=1}^{\infty} \frac{1}{\lambda_n^9} \psi(\lambda_n, \rho, \beta) (1 - e^{-(2\lambda_n^4/3\alpha)t}) \\
 & + I' \sum_{n=1}^{\infty} \frac{1}{\lambda_n^5} \psi(\lambda_n, \rho, \beta) (1 - e^{-(2\lambda_n^4/3\alpha)t}),
 \end{aligned} \tag{A15}$$

Equations (A14) and (A15) represent the complete solution for the velocity and displacement of the plate. In the limit as $\beta \rightarrow 0$, the Gaussian ideal impulse becomes the uniform ideal impulse and this solution reduces to the solution presented by Wierzbicki (ref. 12).

REFERENCES

1. Perzyna, P.: Dynamic Load Carrying Capacity of a Circular Plate. *Arch. Mech. Stos.*, Vol. 10, No. 5, 1958, pp. 635-647.
2. Weidman, D. J.: Response of a Plastic Circular Plate to a Distributed Time-Varying Loading. Ph. D. Thesis, Virginia Polytechnic Institute and State University, 1968.
3. Youngdahl, C. K.: Influence of Pulse Shape on the Final Plastic Deformation of a Circular Plate. *Int. J. Solids Structures*, Vol. 7, 1971, pp. 1127-1142.
4. Florence, A. L.: Annular Plate Under a Transverse Line Impulse. *AIAA Journal*, Vol. 3, No. 9, 1965, pp. 1726-1732.
5. Sneddon, I. E.: Fourier Transforms. McGraw-Hill Book Co., Inc., 1951, pp. 145-147.
6. Madden, R.: Ballistic Limit of Double-Walled Meteoroid Bumper Systems. NASA TN D-3916, 1967.
7. Thomson, R. G.: Plastic Behavior of Circular Plates Under Transverse Impulse Loadings of Gaussian Distribution. NASA TR R-279, 1968.
8. Perzyna, P.: The Constitutive Equations for Work-Hardening and Rate Sensitive Plastic Materials. *Proc. Vib. Problems*, Vol. 4, 1963, pp. 281-290; *Bull. Acad. Polon. Sci., Ser. Sci. Tech.*, Vol. 12, 1964, pp. 199-206.
9. Hohenemser, K.; and Prager, W.: Über die Ansätze der Mechanik isotroper Konitinua. *ZAMM*, Vol. 12, 1932, pp. 216-226.

10. Prager, W.: Mécanique des solides isotropes au delà du domaine élastique. *Memorial Sci. Math.* 87, Paris, 1937, Eq. (47) on p. 27.
11. Perzyna, P.: Fundamental Problems in Viscoplasticity. *Advances in Applied Mechanics*. Vol. 9, 1966, pp. 202-243.
12. Wierzbicki, T.: Impulsive Loading of Rigid Viscoplastic Plates. *Int. J. Solids Structures*, Vol. 3, 1967, pp. 635-647.
13. Florence, A. L.: Circular Plate Under a Uniformly Distributed Impulse. *Int. J. Solids Structures*, Vol. 2, 1966, pp. 37-47.
14. Wierzbicki, T.: A Method of Approximate Solution of Boundary Value Problems for Rigid, Viscoplastic Structures. *Acta Mechanica*, Vol. 3, No. 1, 1967, pp. 56-66.
15. Hayduk, R. J.; and Thomson, R. G.: Static Load-Carrying Capacity of Circular Rigid-Plastic Plates Under Gaussian Distribution of Pressure. *Int. J. of Solids and Structures*, Vol. 12, 1976, pp. 555-558.
16. Wang, A. J.: The Permanent Deflection of a Plastic Plate Under Blast Loading. *J. Appl. Mech.*, Vol. 22, No. 3, 1955, pp. 375-376.

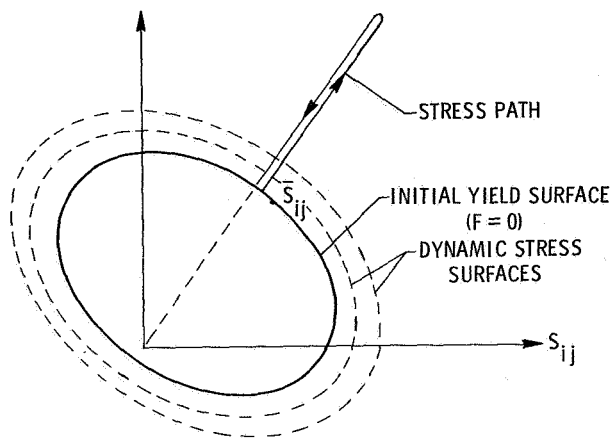


Figure 1.- Representation of proportional loading in deviatoric space.

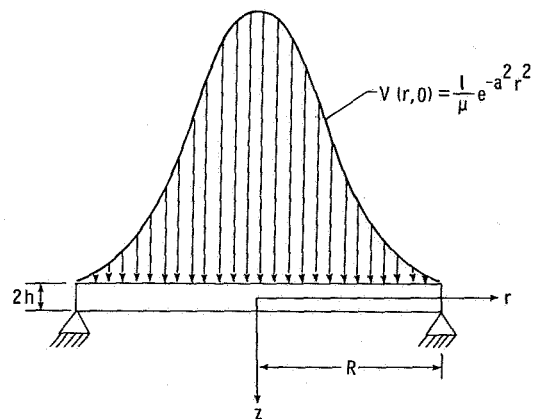


Figure 2.- Simply supported circular plate with Gaussian distribution of initial velocity.

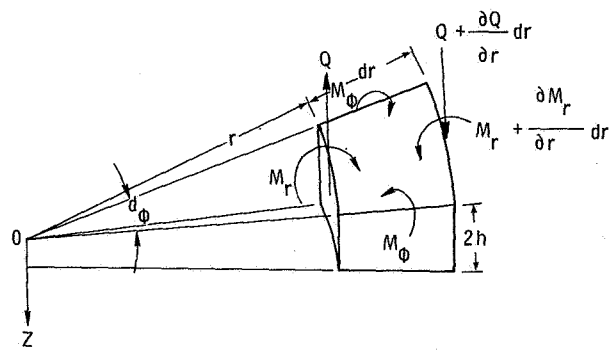


Figure 3.- Element of the circular plate with internal forces and moments.

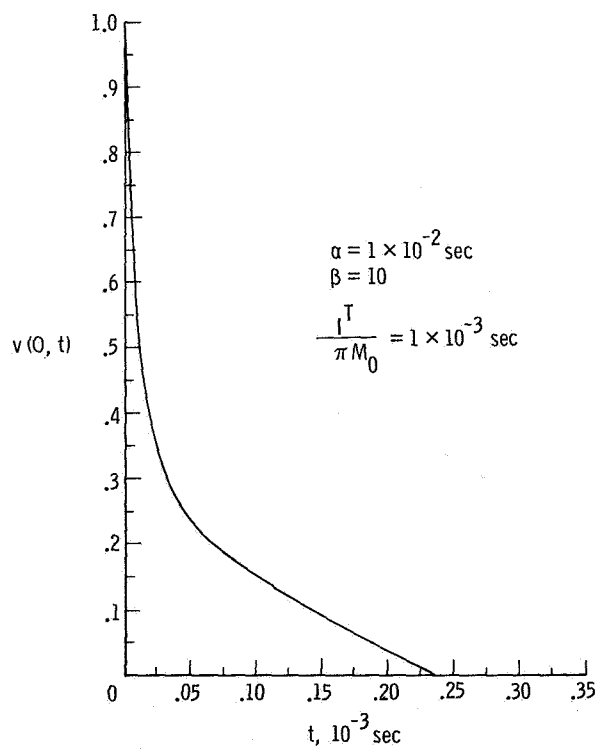
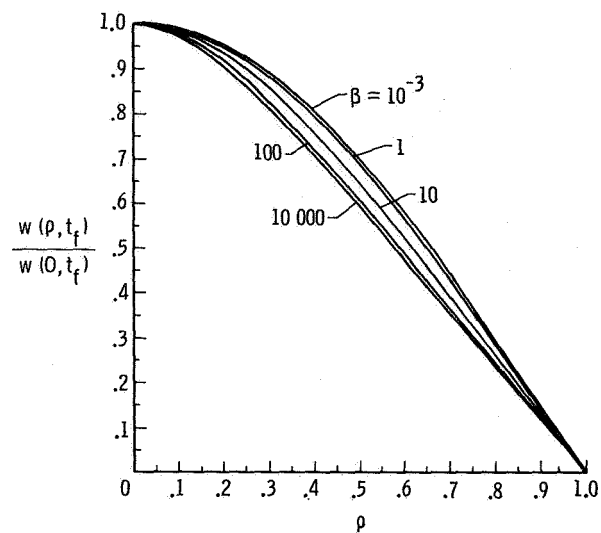
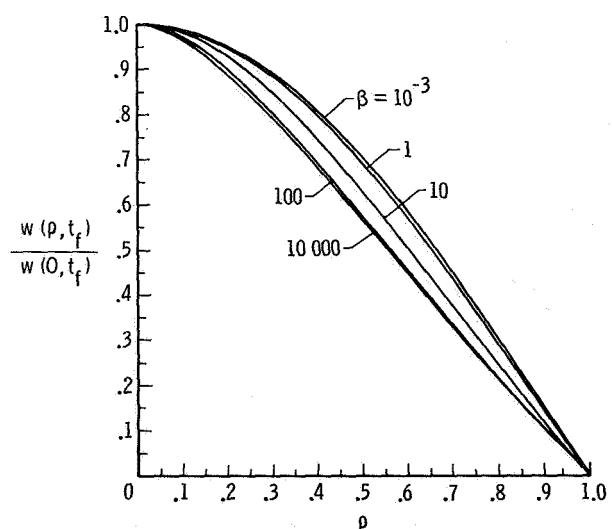


Figure 4.- Representative time history of plate central velocity for the Gaussian ideal impulse loading.



(a) $\alpha = 1 \times 10^{-3}$ sec.



(b) $\alpha = 1 \times 10^{-2}$ sec.

Figure 5.- Final plate profiles for various values of the ideal impulse shape parameter, β .

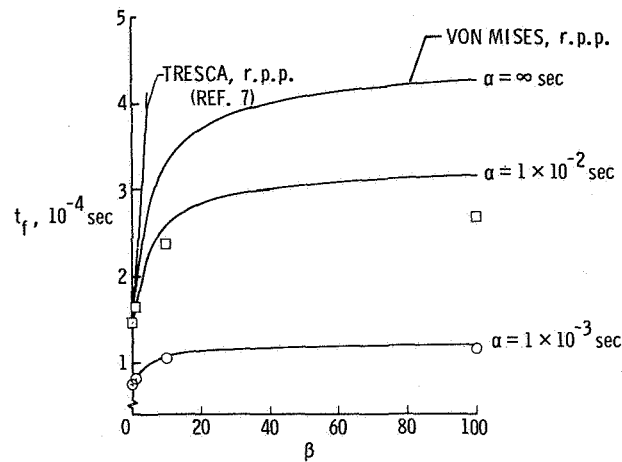


Figure 6.- Comparison of approximate expression (eq. (22)) for motion to cease, t_f , and points determined from the complete equations for the ideal impulse loading.

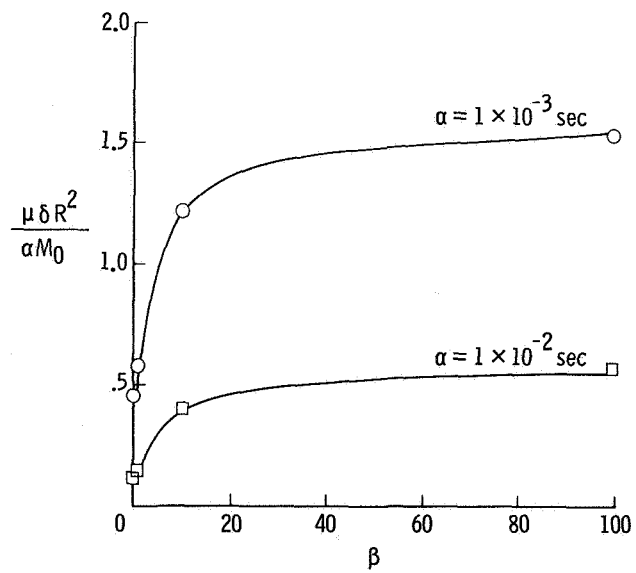


Figure 7.- Comparison of approximate expression (eq. (25)) for the final central deflection and points determined from the complete equations for the ideal impulse loading.